Additive Manufacturing

HEAT TREATMENTS FOR IMPROVED QUALITY BINDER JETTED MOLDS FOR CASTING ALUMINUM ALLOYS.
--Manuscript Draft--

Title:

HEAT TREATMENTS FOR IMPROVED QUALITY BINDER JETTED MOLDS FOR CASTING ALUMINUM ALLOYS.

Authors:

P. Rodríguez-González; A.I. Fernández-Abia; M.A. Castro-Sastre; J. Barreiro.

University of León, Department of Mechanical, Informatics and Aerospace Engineering. Campus de Vegazana, 24071 León, Spain.

Corresponding autor:

A. I. Fernández-Abia, aifera@unileon.es, Tel. +34987291984

Declaration about other concurrent submissions:

By the present the authors declare that there is no other previous or concurrent submission to other journals or congresses. The content of the paper is original and reproduces the research work done by the authors.

Professional proofreading
The paper has been professionally proofread.

30 March 2020

To whom it may concern,

RE: Proof-Reading-Service.com Editorial Certification

This is to confirm that the document described below has been submitted to Proof-Reading-Service.com for editing and proofreading.

We certify that the editor has corrected the document, ensured consistency of the spelling, grammar and punctuation, and checked the format of the sub-headings, bibliographical references, tables, figures etc. The editor has further checked that the document is formatted according to the style guide supplied by the author. If no style guide was supplied, the editor has corrected the references in accordance with the style that appeared to be prevalent in the document and imposed internal consistency, at least, on the format.

It is up to the author to accept, reject or respond to any changes, corrections, suggestions and recommendations made by the editor. This often involves the need to add or complete bibliographical references and respond to any comments made by the editor, in particular regarding clarification of the text or the need for further information or explanation.

We are one of the largest proofreading and editing services worldwide for research documents, covering all academic areas including Engineering, Medicine, Physical and Biological Sciences, Social Sciences, Economics, Law, Management and the Humanities. All our editors are native English speakers and educated at least to Master's degree level (many hold a PhD) with extensive university and scientific editorial experience.

Document title: HEAT TREATMENTS FOR IMPROVED QUALITY BINDER JETTED MOLDS FOR CASTING ALUMINUM ALLOYS

Author(s): P. Rodríguez-González; A.I. Fernández-Abia; M.A. Castro-Sastre; J. Barreiro.

Format: American English

Style guide: Additive Manufacturing at https://www.elsevier.com/journals/additive-manufacturing/2214-8604/guide-for-authors

HEAT TREATMENTS FOR IMPROVED QUALITY BINDER JETTED MOLDS FOR CASTING ALUMINUM ALLOYS.

Abstract

The objective of this paper was to investigate the most suitable heat treatment for casting molds manufactured by binder jetting. For this purpose, the printed molds were subjected to different heat treatments and the properties of the molds were analyzed. Tests were performed at different temperatures and times to investigate their effect on the water and volatile substances content; the joining among particles; and the porosity, roughness, and compression strength of the printed molds. Moreover, to relate the properties of the mold with the quality of the castings, aluminum alloy specimens were cast and the dimensional accuracy, surface roughness, mechanical strength, and porosity were evaluated. This research leads to the conclusion that the binder jetting process, using calcium sulfate powder, is useful for manufacturing molds for casting aluminum alloy. To improve the mold quality and, consequently, the casting quality, heat-treatment is necessary. The best mold properties were obtained at 250°C for 1.5 hours.

Keywords: Additive manufacturing; Binder jetting; Aluminum casting; Mold properties; Calcium sulfate.

1. Introduction

Additive manufacturing (AM) technology was originally conceived for producing rapid prototypes. Today, this technology has many applications offering solutions in several industrial sectors, from biomedical to aerospace applications. Several AM processes, especially binder jetting, have been used for metal casting, reducing cost and time. This technique is a powder-based process that uses a binder to join powder particles, layer by layer. The process starts spreading a layer of powder onto a platform using a roller. Then, a print-head injects a binder liquid to join the powder particles in certain areas, according to the part design in CAD. To continue with the three-dimensional printing process, the platform descends a distance equivalent to the layer thickness and spreads a new layer of powder. The print-head again injects binder liquid to join powder particles selectively. This process is repeated until the complete part is printed. The part obtained is called a "green part" and it is usual to perform post-treatments to improve the final properties.

A complete mold with complex internal geometries can be manufactured, directly from the CAD model, using this technique; it avoids the fabrication of pattern and core boxes and integrates gating system and cores directly into the mold [1]. Sarojrani et al. [2] reviewed developments in the investment casting process and highlighted the advent and emergence of rapid prototyping using different rapid prototyping processes, analyzing their advantages and limitations. In Le Néel et al.'s review [3] it was revealed that binder jetting for sand casting provides an excellent solution to the casting industry, although more studies need to be done for optimizing metal casting

applications. Using the binder jetting technique, the mold can be reduced to a shell a few millimeters thick, improving the yield of the mold [4]. Additionally, the reduction of mold thickness results in a faster cooling rate of the molten metal, therefore, affecting the mechanical properties of the castings [5]. Shangguan et al. [6] designed a shell-truss sand mold with a geometry that allows controlling the cooling rate at different casting areas. Although the mold has a complicated shape, it can be printed thanks to the freeform fabrication typical of binder jetting. Additionally, the required amount of sand was reduced by two-thirds per mold compared to a traditional dense sand mold. Other researchers also illustrated the advantages of using binder jetting to produce molds using non-conventional designs [7]. Without any geometric limitation, each element of the rigging system (e.g. pouring basin, sprue, and runners) can be redesigned to improve casting performance. Optimized gating designs result in lower turbulence, fewer oxide films, and less air entrapment during mold filling. Kang et al [8] proposed a skeletal mold, featuring a lattice-shell and rib enforced shell, to achieve fast and uniform casting cooling. The mold design allows adjusting the cooling and solidification conditions of particular casting zones. This type of mold with complicated shapes can be made by a binder jetting process, improving production efficiency and reducing deformation, residual stress, and casting defects.

Binder jetting can use a wide variety of powder and binder materials. Upadhyay et al. [9] reviewed binder jetting for rapid sand casting and found that the materials commonly used to print molds for casting applications are silica, zircon, chromite, plaster-ceramic composite, and ceramic beads. These materials use organic binders and furan resins to bind the powder particles. The disadvantage of organic binders is the toxic gas generation during casting. Furan resins are carcinogenic and, therefore, harmful to operators. These aspects lead to important limitations, and alternative materials are necessary to make environmentally friendly foundries. As it is known, the base mold material and binder are the most important factors to obtain quality castings. Snelling et al. [10] studied the effect of different materials on cast material properties. For this purpose, the material properties of A356-T6 castings were compared for different mold materials. Two molds were fabricated by binder jetting, using ZCast® (produced by 3D Systems) and ExOne silica sand (produced by ExOne Company). The castings were compared against traditional no-bake sand. Castings from ExOne molds had more quality. ZCast® molds produced lower quality castings because of gas defects associated with a high quantity of binder and low mold permeability due to small grain size.

Binder jetting using calcium sulfate hemihydrate powder (commercial name Visijet PXL Core by 3DSystems) can be used for foundry application to print molds for non-ferrous castings. This material uses a water-based binder solution of 2-Pyrrolidone [11]. Therefore, the toxic gas generation is restricted, reducing environmental damage. Currently, this material is used mainly for medical and dental applications. In the medical field, it is widely used for producing synthetic scaffolds for tissue engineering. Many studies have been conducted to improve the required final properties of printed scaffolds [12, 13].

Even though binder jetting can manufacture molds with complex geometries, there are still restrictions that prevent obtaining quality castings. To obtain a high casting quality, the mold must have high permeability, low water and volatile content, good dimensional accuracy, and adequate compressive strength to withstand the pressure exerted by the molten metal inside the mold cavity. A mold manufactured directly through 3D printing does not have all these good properties. Consequently, it is necessary to post-process the mold to optimize the structure and mechanical properties to improve the strength, porosity and surface roughness. The properties of binder jetting printed parts can be controlled by different factors, such as printing parameters (printing speed, layer printing delay, and layer thickness), powder parameters (particle size, composition, humidity, flowability, and wettability), and binder parameters (concentration, activator content, and binder type). In addition, it is also possible to improve the properties of green parts by thermal treatment. Several studies have been focused on various of these parameters. Vaezi et al. [14] studied the effects of layer thickness and binder saturation level on mechanical strength, integrity, and dimensional accuracy in the binder jetting process. They concluded that increasing binder saturation led to specimens with higher strength and integrity. Additionally, decreasing layer thickness increased the tensile strength and decreased the flexural strength, among other findings. Another study [15] was focused on the effect of print resolution, recoater speed, and job box position on the permeability and the strength of sand molds. A statistical analysis of the results revealed that a higher recoater speed leads to higher permeability and less strength due to minor powder compaction. On the other hand, a fast recoater speed leads to anisotropic properties in the sand specimens within a given job box. Finally, the print resolution only affects mold strength. Patirupanusara et al. [16] studied the influence of adhesive binder content on the formability and the physical and mechanical properties of fabricated binder jetting samples. Butscher et al. [17] analyzed the relationship between key powder parameters (particle size, flowability, roughness, and wettability) and printing accuracy. Other researchers [18] incorporated sisal fibers into gypsum powder to produce stronger composite printed parts.

Researchers have also focused on thermal treatments. Several works revealed that curing parameters (temperature and time) modify the properties of printed parts, such as strength and permeability. Mitra et al. [19] undertook a deep investigation to understand the relationship between the amount of binder present in the binder jetting mold and the three-point bending strength and permeability. The modification of these properties is related to the reactions that the binder undergoes under certain conditions of temperature and time. The increase in strength may be related to solvent evaporation, which causes shortening and hardening of resin bridges. The variation in permeability during binder evaporation is a result of a combination of two effects: (i) shrinkage, due to shortening resin bridges, leading to lower permeability; (ii) an increase in pore size that may occur due to evaporation of the binder, leading to a higher permeability. Therefore, when increasing the temperature, the permeability of the printed specimen decreases, as shrinkage is the dominant mechanism. Bassoli and Atzeni [20] carried out an experimental study to evaluate the mechanical and dimensional changes induced by different thermal treatments. They concluded that curing time is almost irrelevant for the compression strength whereas temperature has

a significant effect. They also concluded that dimensional accuracy is almost independent of the thermal treatment applied.

All these studies focused on the properties of the molds produced by binder jetting processes, but few works analyze the relationship between the casting quality and the mold properties. In our research, binder jetted molds were optimized for aluminum casting parts. The molds were thermally treated at various heating conditions to improve their capability for the casting process. In addition, the quality of casting parts obtained with these thermally treated molds was studied. Section 2 presents the experimental procedure and the results of the thermal treatment for the binder jetting mold. In Section 3, the aluminum casting part quality is analyzed. Section 4 presents the conclusions.
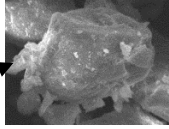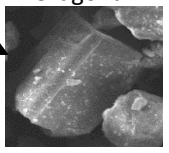
2. Thermal treatment for binder jetting molds

The first goal of this research is to establish the most suitable thermal treatment for binder jetting molds. Different analyses were carried out to determine the appropriate temperature and time ranges for thermal treatments. Differences in the properties of thermal-treated binder jetting molds were analyzed in terms of surface roughness, porosity and compression strength for several heating conditions. Section 2.1 explains the experimental procedure to determine the thermal treatments applied to the as-manufactured molds. The results obtained are shown in Section 2.2.

2.1. Experimental procedure to determine the thermal treatment for binder jetting molds

2.1.1. Materials

The material used to print the mold was a commercial plaster-based powder, $CaSO_4$ ½ H_2O (commercial name VisiJet PXL Core, from 3DSystems) with 80–90%purity, with a water-based binder solution (commercial name VisiJet PXL Clear). Both materials are used in a 3D printer machine, ProJet CJP 660Pro (3DSystems). The characterization of the powder and the binder were carried out by the authors in a previous work [11]. Table 1 shows the chemical composition and phases found in the $CaSO_4$ $_nH_2O$ system and the bassanite structure.

Table 1. Powder characterization: Chemical composition (EDX), Calcium sulfate phases (identified by Raman Spectroscopy and calculated based on the XRD), and Basanite structure (according to pdf ICCD letters) [11]

Chemical composition		Phases in CaSO$_4$ nH$_2$O system		Structure
Element	% Weight	Phases	% Weight	Orthorhombic
O	40,31	CaSO$_4$ 2H$_2$O (Gypsum)	0,7	
S	13,79			
Ca	17,89			
C	28,01	CaSO$_4$ ½ H$_2$O (Bassanite)	60,9	
Na	0,28		35,1	Hexagonal
Al	0,29			
Mg	0,95			
Si	1,40	CaSO$_4$ (Anhydrite)	3,2	
K	0,67			

The composition of the water-based binder solution is 1% 2-Pyrrolidone (C$_4$H$_7$NO) with impurities. Table 2 shows the chemical composition of impurities in the binder, found using ICP-OES. These impurities were added to accelerate the powder's bonding mechanism.

Table 2. Chemical composition impurities in the binder (ICP-OES mg/l) [11]

Analyte	Mg (285,213)	Na (589,592)	K (766,490)	Al (396,153)
Binder (mg/l)	0,13	73,20	2,24	<0,10

According to this information, humidity and volatile substances, coming from the binder, are found in the parts in the as-printed state (directly from the 3D printer), as are impurities coming from the powder material. Therefore, it is necessary to apply a heat treatment to the molds to eliminate the water, volatile substances, and impurities. So, the problem of gas generation during casting is avoided, minimizing defects in the molded parts.

2.1.2. Thermogravimetric analysis

A thermogravimetric analysis (TGA) was carried out for a deeper understanding of the reactions that take place between the powder and the binder as temperature changes. This analysis allows knowing thermal behavior and the temperature ranges in which mass loss occurs for the material components. TGA was carried out using a TA Instruments model Q600. To obtain the curves, 20 mg samples were 3D-printed. It was performed at a 5 °C/min heating rate in air and in a temperature range between 25 and 600°C. This analysis allowed us to set the temperature limits for heat treatments.

2.1.3. Weight loss analysis varying the temperature and curing time

To determine the second parameter of the thermal treatment, the curing time, the weight loss of the specimens manufactured for this purpose was examined. A set of tests was carried out varying the temperature in a range between 150 and 300°C (according to the results obtained in the previous TGA analysis) and the time in a range between 1 and 5 hours, as indicated in Table 3. Rectangular specimens were 3D-printed for these tests. The specimen dimensions were 35 x 35 mm with a 5 mm

thickness. The 5 mm thickness was defined to keep the analysis conditions similar to the binder jetting molds.

Table 3. Thermal treatment parameters.

Parameter	Values					
Temperature (°C)	150	200	250	300		
Time (h)	1	1,5	2	3	4	5

Three repetitions were done for each combination of parameters. Measurements were taken using a balance with a 0.01 g measuring accuracy for each sample before and after the heat treatment. The weight after the treatment was compared with the weight before the treatment. The weight loss, expressed in percentage, was calculated according to Equation 1.

$$\% \, Weight \, loss = \frac{Initial \, weight - Final \, weight}{Initial \, weight} x \, 100 \qquad (1)$$

As a result of both previous studies (TGA and weight loss), three different conditions were chosen for the heat-treating the binder jetting molds, designated as T1, T2, and T3.

2.1.4. Roughness measurement

To evaluate the surface quality of the heat-treated samples, surface roughness was measured using a Mitutoyo Surftest SJ-500 profilometer. The average roughness (R_a) parameter was calculated according to ISO 4288:1996 [21]. The measures were taken in different areas and directions on the samples.

2.1.5. Porosity

Apparent porosity measurements were performed using the Archimedes method according to ASTM C373-88 [22]. For this purpose, five specimens were 3D-printed for each of the thermal treatments (T1, T2, and T3). Additionally, five specimens were preserved without any heat-treatment (green samples) for comparison. The sample shape was a cube with an approximately 60 g weight following the indications of the ASTM standard. The immersion fluid used for the test was toluene with a density ρ_l= 0,864 g/cm^3. This liquid was used because calcium sulfate is not soluble in toluene and it presents low surface tension (23.3 mN/m at room temperature). A balance with a 0.01 g measuring accuracy was used to weigh the specimens.
The apparent porosity, P, expressed as a percentage, was calculated using Equation (2), where M is the saturated mass, D is the dry mass, S is the mass of the specimen while suspended in toluene, and ρ_l is the density of toluene.

2.1.6. Compression tests

Compression tests were carried out following the ISO 679:2009 standard [23] using a compression testing machine (Ibertest MD2 W). To investigate the anisotropic behavior in relation to part building orientation, the force was applied in different directions. Anisotropic behavior may be due to differences in the joining of particles in

the same layer and between layers. For this purpose, a compressive force was applied parallel to the direction of the printed layers, the X-axis (print-head direction) and Y-axis (re-coater direction), and perpendicular to the direction of the printed layers, Z-axis, as indicated in Figure 1.
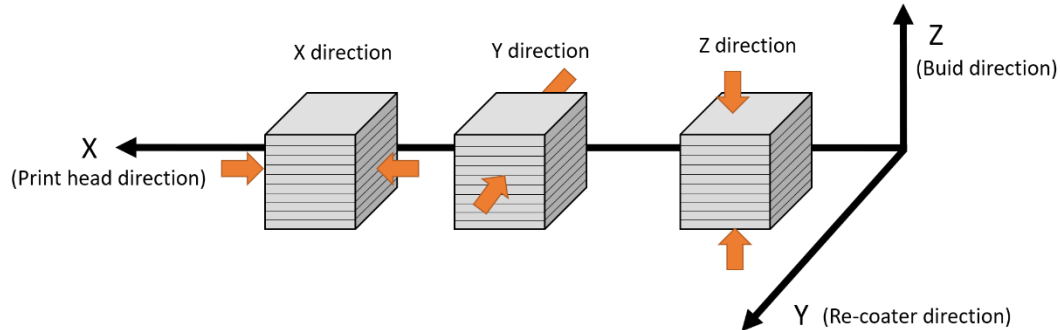

Figure 1. Direction of compression force.

The compression tests were carried out on samples with the three thermal treatments (T1, T2, and T3) and on samples without thermal treatment. Three specimens (40 mm x 40 mm x 50 mm) were tested for each condition. During the test, a uniformly increasing load was applied at 50 ± 10 N/s until the sample broke, obtaining the compressive strength.

## 2.2.	Results and discussion about thermal treatments for binder jetting molds
## 2.2.1.	Thermogravimetric analysis

Figure 2 shows the thermogravimetric curve and its derivative curve corresponding to the mixture of powder and binder. A total mass loss of 16.88% was observed from room temperature to 600°C in three clear weight loss steps.
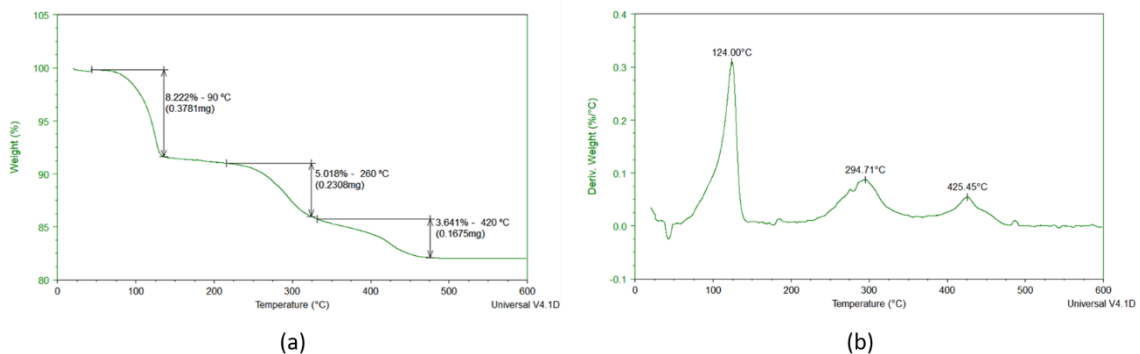

Figure 2. Thermogravimetric curve (a) and derivative curve (b) of powder and binder.

The mass loss of the material was continuous, starting from the beginning of the heating cycle, as shown in Figure 2.

The greatest loss of mass takes place during the first step of dehydration (8.222% weight loss from room temperature to 140°C), reaching a maximum value at 124°C. It could be attributed to the loss of residual water (drying process) and the conversion of $CaSO_4 \cdot 2H_2O$ to $CaSO_4 \cdot 1/2H_2O$ and $CaSO_4 \cdot 1/2H_2O$ to $CaSO_4$ [24].

In the next step (140 to 325°C), the change in mass was 5.018%. This loss could be mainly attributed to two processes: (i) water loss due to the following transformation ($CaSO_4. 2H_2O \rightarrow CaSO_4. 1/2H_2O \rightarrow CaSO_4$) and (ii) weight loss due to burning the organic elements in the binder (2-pyrrolidone; boiling point 245°C) and powder.

The last step (325 to 475°C) led to a mass loss of 3.641%. The maximum occurred at 425.25°C. This mass loss could be attributed to three phenomena: (i) the elimination of internal water in the bassanite structure, (ii) the completion of water molecule removal and the formation of anhydrite, (iii) the sulfate transforming into calcium oxide and calcium sulfur with the loss of SO_2 and SO_3 gases generated during the transformation. This transformation was verified by the EDX analysis. The images in Figure 3 show variations in the O/S, Ca/S, and O/Ca ratios. The EDX-ray spectrum derived from the general area (X30) shows peaks for oxygen, sulfur, and calcium (Figure 3 a).
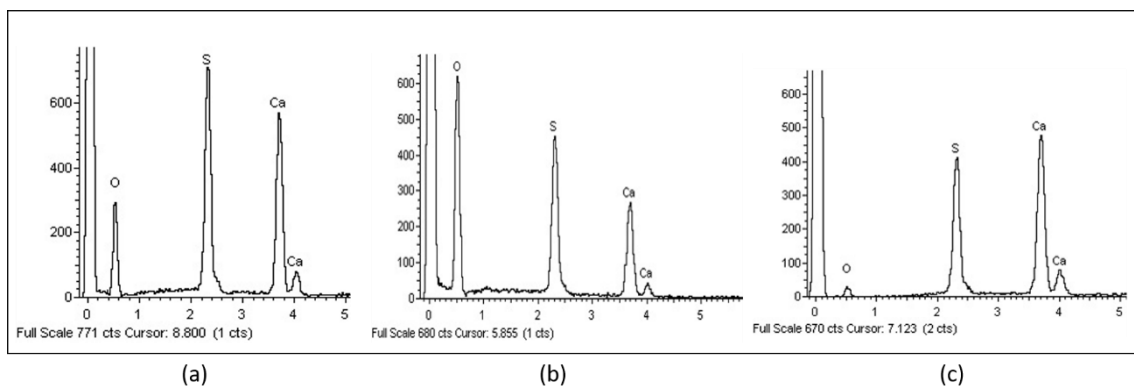
Figure 3. EDX-ray spectra at different magnifications and areas: (a) general area of the printed part (X30) (b) smaller area on the printed part (X9000) (c) smaller area on the printed part (X95000)

Changes in peak intensities related to oxygen, sulfur, and calcium, which appear in the RX spectra obtained at a greater magnification (Figure 3b and 3c), show the sulfate decomposition at these temperatures. The higher intensity of the oxygen peak with respect to the sulfur and calcium peaks (Figure 3b) suggests the formation of calcium oxide; the lower intensity of the oxygen peak in the X-ray spectra (Figure 3c) suggests the partial conversion of calcium sulfate into calcium sulfur.

The information obtained in this analysis leads to limiting the temperature range to perform a thermal treatment on the printed mold. The temperature range was established between 150°C and 350°C. The lower value was established because, at this temperature, the elimination of free water and additives has already occurred (according to TGA results, the maximum loss takes place at 124°C). The upper limit (350°C) was established because, at this temperature, a high percentage of internal water and gases have been eliminated. At higher temperatures, reactions take place that degrade the material, decreasing the bond between particles and, therefore, reducing the material strength, as verified with the compression tests.

2.2.2. Weight loss analysis varying temperature and curing time

Figure 4 shows the weight loss as a function of curing time at different temperatures. As expected, a weight loss is seen for all thermal-treated samples. The weight loss is greater for the specimens heated at the highest temperatures.
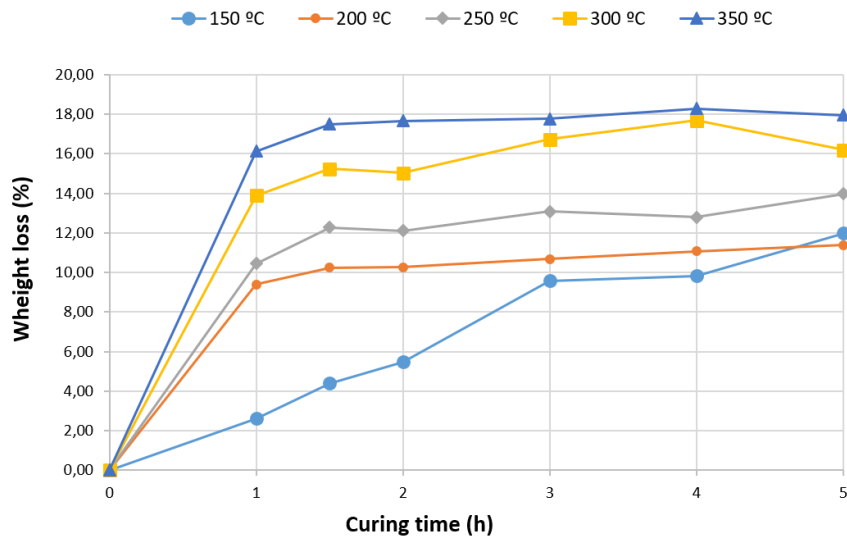

Figure 4. Weight loss with curing time for different temperatures.

For all temperatures, except 150°C, the rate of weight loss is high up to 1.5 hours and it keeps almost constant later. However, at the lowest temperature (150°C), the weight loss increases linearly up to 3 hours, keeping constant after. This trend is consistent with the TGA results. Considering this behavior, the curing time must be 3 hours for 150°C. A lower curing time does not ensure that all the free water and impurities have been removed, as indicated by the slope of the curve at 150°C. At higher temperatures, a curing time of 1.5 hours is enough. Heating the material for a longer time does not provide any advantage in terms of removing undesirable elements. On the other hand, increasing the heating time implies higher cost and energy consumption.

As a result of both analysis (TGA and weight loss), three different conditions were chosen for thermally treating binder jetting molds, based on the material composition and economic criteria. These conditions are 150°C for 3 hours, 250°C for 1.5 hours and 300°C for 1.5 hours (Table 4).

Additional differences of binder jetting printed specimens were studied when applying these three heat-treatment conditions and no thermal-treatment (green), analyzing roughness, porosity, and compression strength.

Table 4. Thermal conditions for binder jetting molds.

Thermal-treatment designation	Conditions
Green	No thermal-treatment
T1	150 °C for 3 hours
T2	250 °C for 1,5 hours
T3	300 °C for 1,5 hours

2.2.3. Surface roughness of binder jetting thermal-treated samples

The surface roughness of the mold directly affects the roughness of the casting, since the molten metal fills mold surface interstices caused by the join among powder grains. In addition, other factors influence casting roughness, such as the pouring temperature [25] and the wetting properties of the metal alloy [26]. In our study, there are no significant differences in roughness when applying different heat treatments, according to the results indicated in Figure 5. Roughness values for all thermal-treated samples are consistent with values allowed for casting molds.
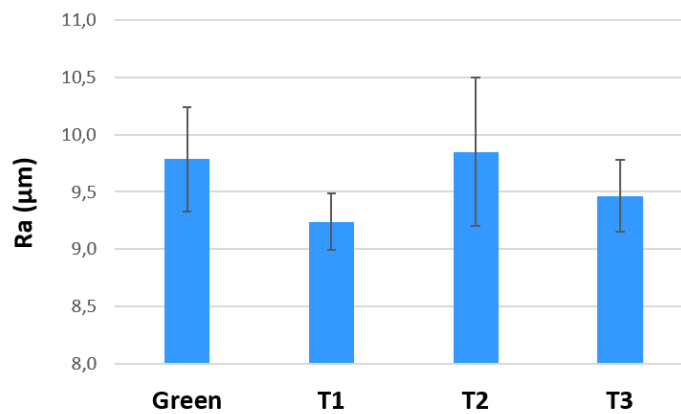

Figure 5. Roughness for the binder jetting thermal-treated samples

2.2.4. Porosity of binder jetting thermal-treated samples

The heat treatment causes the evaporation of water and volatile substances. This phenomenon leads to an increase in mold porosity, therefore affecting the quality of the castings. Porosity was measured using the Archimedes method. The results indicate that porosity is higher for the thermally treated samples than for the green samples. Also, porosity increases at higher temperatures (Figure 6).
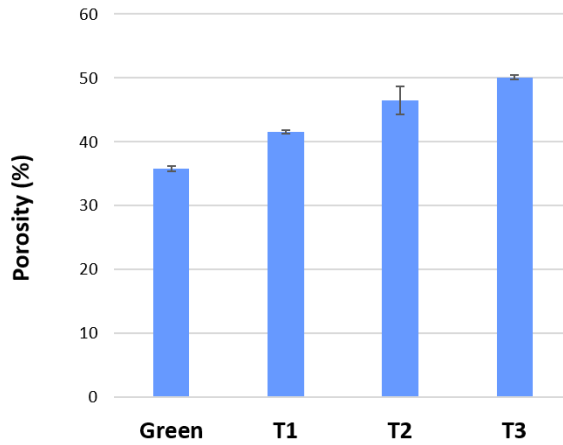
Figure 6. Porosity for the binder jetting thermal-treated samples

On one hand, a high porosity facilitates the evacuation of gases trapped in the cavities when the metal is poured, therefore avoiding casting defects. On the other hand, when increasing porosity, mechanical strength decreases [27]. Molds with low mechanical strength do not withstand the metallostatic pressure and the mold could break. Therefore, a balance between porosity and strength is required.

2.2.5. Compression tests for binder jetting thermal-treated samples

As mentioned, an important feature of a mold is the mechanical strength to withstand the pressure caused by the metal when filling the cavity. The molten metal tends to compress the walls of the mold. Therefore, it is necessary to evaluate the compression strength. This value will also allow establishing the minimum wall thickness of the mold to withstand the stresses without cracking or breaking down.
The results of the compression tests showed that the orientation does not significantly affect the mechanical behavior of the printed parts. Average values for compression strength are shown in Figure 7 for different force directions (X, Y, and Z). The values were similar for all directions, hence there is not a significant anisotropic behavior.
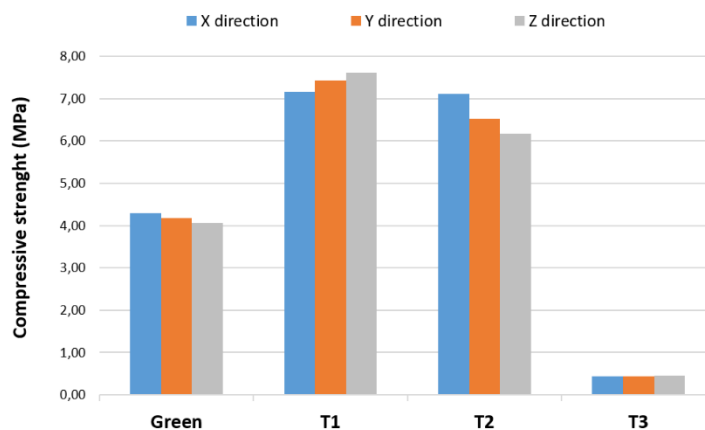

Figure 7. Compressive strength for binder jetting thermal-treated samples

The highest compression strength occurred for specimens with the T1 treatment, with an average value of 7.4 MPa. This value represents an increase of 43% compared to green samples. The compression strength for T2 specimens was slightly lower. The average value was 6.60 MPa, which represents an increase of 37% compared to green samples. T3 specimens, heated to 300°C, suffered an overall loss of strength, with an average value of 0.44 MPa. This phenomenon means that at 300°C, the powder particles are partly detached, and the material degrades due to chemical transformations of the sulfate, according to TGA analysis. The low strength makes the mold unworkable since it does not withstand handling and metal pouring.

This reduction in compression strength was further analyzed using scanning electron microscopy (SEM). SEM micrographs of the thermal-treated specimens' surface are shown in Figure 8a–d. In Figure 8a, powder particles do not show any damage. In contrast, Figures 8b–d show particles with fractures due to different chemical reactions, such as loss of crystallization water, decomposition, and the combustion of elements present in the binder and powder. In the case of the T3 thermal treatment (Figure 8d), the cracks are more severe, causing material breakage and resulting in smaller and detached particles. This thermal degradation leads to a loss of strength in the material.
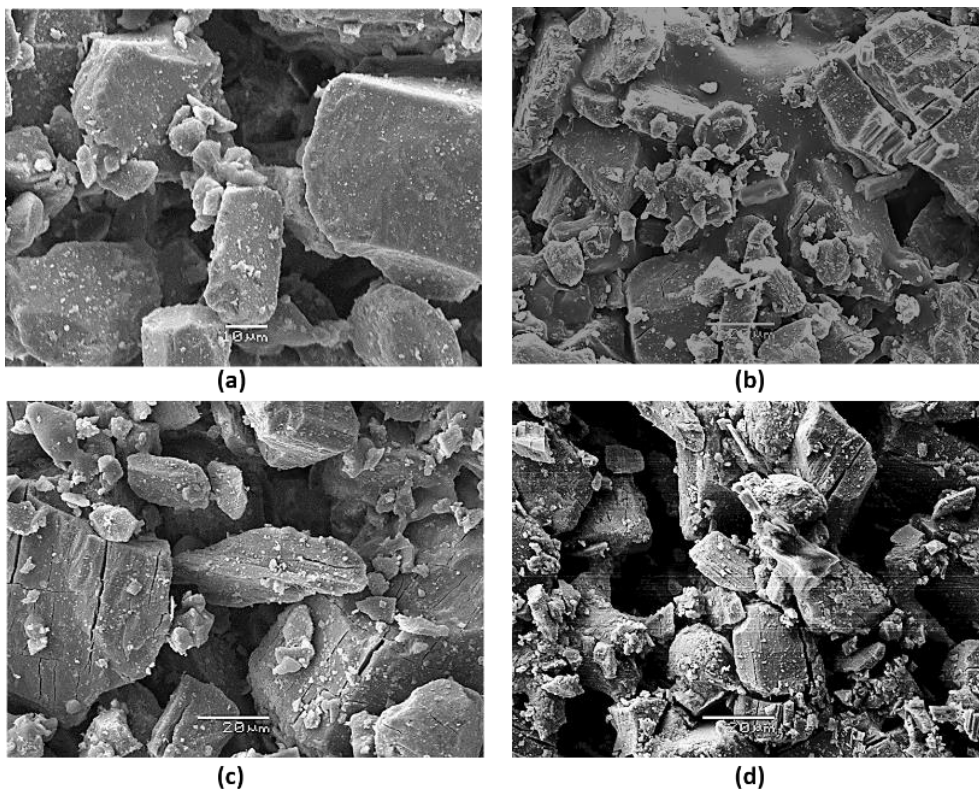
Figure 8. SEM micrographs of samples: (a) without thermal treatment; (b) T1 (150°C for 3 h); (c) T2 (250°C for 1,5 h); (d) T3 (300°C for 1,5 h)

Per the obtained results, the T3 thermal treatment is not suitable because the material begins to degrade and does not have enough strength. Summing up the results, the

most suitable heat treatments for a binder jetting mold are T1 (150°C for 3 hours) and T2 (250°C for 1.5 hours).

3. Quality of aluminum casting parts

The second goal of this research was to analyze the quality of aluminum castings manufactured using the different thermally treated binder jetting molds. The castings were analyzed in terms of dimensional precision, superficial roughness, mechanical strength, and porosity. Section 3.1 explains the tests performed to analyze the quality of aluminum castings. The results obtained are shown in Section 3.2.

3.1. Experimental procedure to analyze the quality of aluminum castings

3.1.1. Manufacturing binder jetting molds and castings

Three molds were manufactured by a binder jetting process using a *ProJet CJP 660Pro* machine from 3DSystems. The mold geometry was designed using CAD software. The molds were designed to cast four specimens for tensile tests. Then, the CAD file was exported to STL format (standard triangle language) to be processed by *3DPrint* software. The result was a mold formed with a 5 mm thick shell, adequate to withstand the pressure produced by the molten aluminum. This thickness saves operation time and cost, according to the results obtained in [28]. Next, three molds were 3D printed using a sulfate-calcium material. After that, one mold was preserved (green reference mold) and the other two molds were thermally treated (T1 and T2). A Hobersal PR/400 muffle was used for this operation. Four specimens were manufactured for each thermal treatment to replicate the tests. The specimen dimensions were defined according to ISO 6892-1:2016 [29].

Once the molds were thermally treated, the next step was to pour the AlSi9Cu3(Fe) aluminum alloy heated to 750°C. Once the aluminum alloy solidified, the castings were extracted from the molds by vibration and crumbling. The riser and gates were cut. Finally, the resultant parts were cleaned with pressurized air to analyze the casting. A summary of the process sequence is shown in Figure 9.
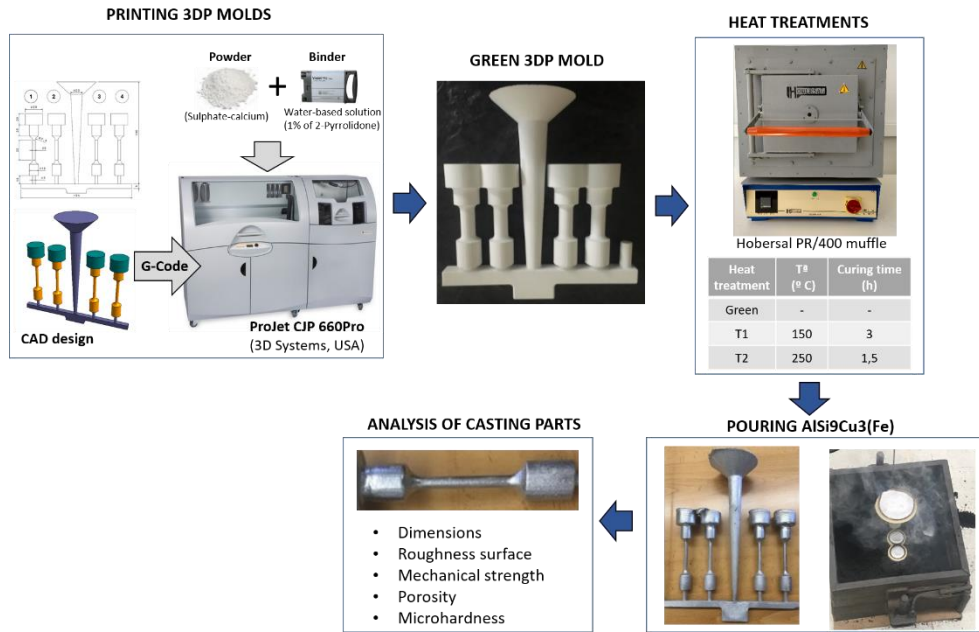
Figure 9. Process sequence for 3D printing the mold and manufacturing the tensile test castings.

3.1.2. Dimensional accuracy and surface roughness of tensile test castings

The castings obtained with the different thermally treated molds were dimensionally measured using a micrometer. Figure 10 shows the dimensions that were evaluated. Four measurements were taken for each dimension and the average value was calculated. Roughness measurements were also acquired on the surface of the specimens, using the same equipment and methodology indicated in Section 2.1.4.
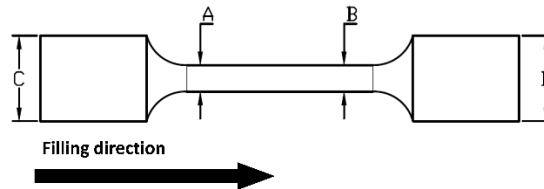

Figure 10. Measured dimensions in the tensile test specimen.

3.1.3. Casting specimen tensile tests

Tensile tests were carried out on 5 mm diameter and 35 mm length circular cross-section specimens, using a universal testing machine and following the ISO 6892-1:2016 standard [29]. Four tensile tests were performed for each thermally treated mold and the ultimate tensile strength (UTS) was recorded for each of them. The average of the four UTS values was considered.

3.1.4. Casting specimen porosities

The porosity of the aluminum parts was calculated using several cross-section micrographs from the middle of the casting. The cross-section surfaces were polished and observed without etching. Metallographic microscopy was used to take micrographs on each sample to cover the total surface. Then, ImageJ software was used to measure the percentage of area with pores.

3.2. Results and discussion about the quality of the aluminum castings

3.2.1. Dimensional accuracy and surface roughness of casting specimens

The accuracy of castings depends on several factors, such as 3D printing machine precision, the thermal treatment applied to the mold, the metal alloy pouring temperature, or the metal alloy shrinkage during solidification. In this study, the focus is only on the thermal treatment of the mold since it is the main objective of the research.

Figure 11 shows the dimensional deviation between the theoretical values (CAD model) and measured values.
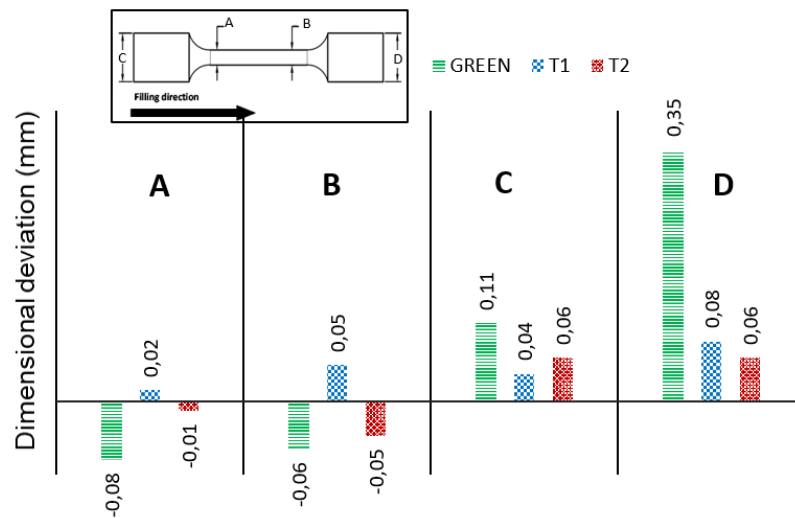

Figure 11. Dimensional deviations (CAD vs Measured values) of castings.

A first visual observation of the results allows noticing that castings manufactured with the green mold exhibit higher deviations for all the measured areas. The dimensional deviations for castings manufactured using both thermally treated molds were quite similar, although precision was slightly better for castings obtained with the T2 thermally treated molds (only dimension C showed a higher deviation).

The head diameter (dimensions C and D) of all casting specimens was smaller than the diameter of the CAD model, whereas deviations for the central diameter (dimensions A and B) showed a different tendency, indicating that mold expansion and deformation act differently depending on the size and the filling zone. Deviations of castings manufactured using the thermally treated molds have very acceptable values, on the order of hundredths of a millimeter.

Roughness values for castings are shown in Figure 12. The value for the casting obtained with the T2 thermal-treated mold is the smallest. This result can be attributed to the lower amount of gases generated in the mold-part interface. A higher gas evacuation was possible due to the greater porosity of the T2 thermally treated mold. The condition of the mold-part interface affects the roughness of castings to a greater extent than the surface state of the mold cavity. From these results, it can be concluded that the three tested molds are acceptable for producing castings, with

roughness values lower than the ones obtained when using the traditional sand-casting process (between 5 and 25 μm Ra) [30].
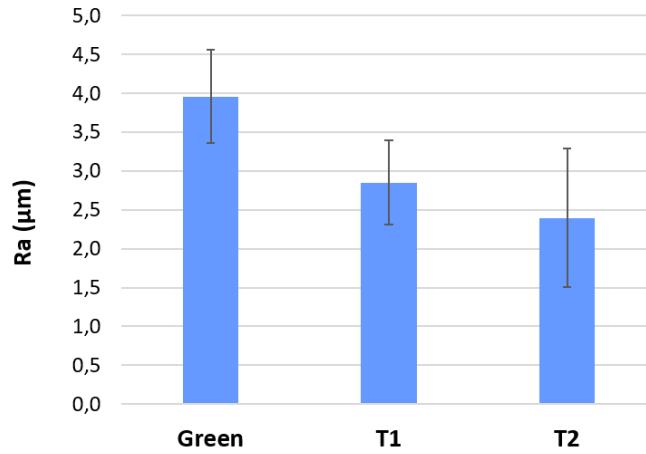

Figure 12. Surface roughness of the castings.

3.2.2. Casting specimen tensile tests

The results obtained in the tensile tests indicate that the three binder jetting thermally treated molds allow obtaining aluminum castings with mechanical properties comparable to traditional casting [31]. Figure 13 shows the ultimate tensile strengths (UTS) of the casting specimens. The UTS values for the specimens manufactured with the T1 thermal-treated mold are significantly lower. This result is contradictory to the general acceptance that an increase in porosity decreases mechanical properties. In the next section, where the porosity is analyzed, the results indicate that the highest porosity value corresponds to samples obtained with the green molds. However, several studies by other researchers, who have analyzed the influence of porosity on mechanical properties in-depth, have shown that there are other factors, such as the shape, type, and distribution of pores, as well as the presence of pores in the fracture area, that have greater influence on fracture behavior and the UTS values [32, 33].
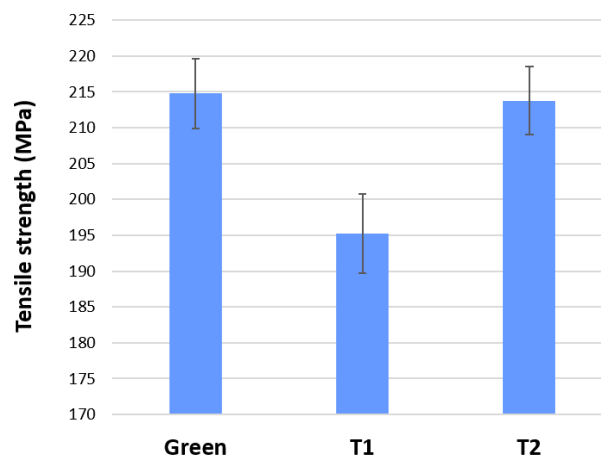

Figure 13. Ultimate tensile strengths (UTS) of casting specimens.

3.2.3. Casting specimen porosities

Figure 14 shows the porosity of the castings manufactured with the three binder jetting thermally treated molds. Based on the shape of pores, it can be concluded that both gas and shrinkage porosities are present.

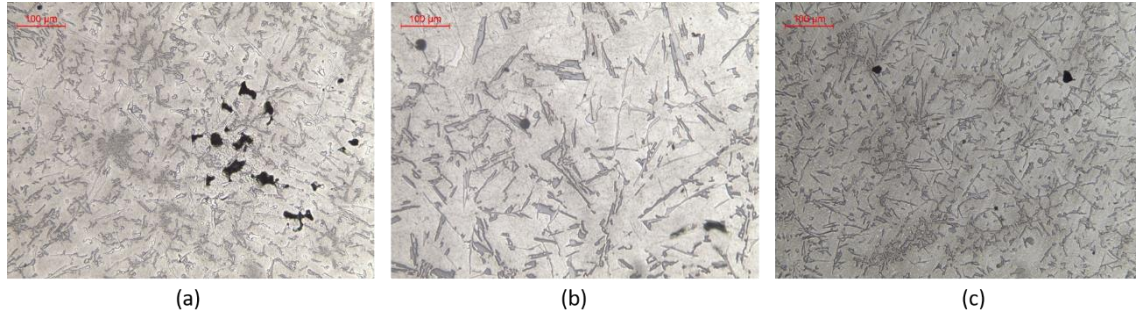(a)   (b)   (c)

Figure 14. Optical microstructures showing the porosity of castings manufactured with the three binder jetting thermally treated molds: (a) Green mold, (b) T1 mold and (c) T2 mold

The results of porosity measurements are indicated in Table 5. The area occupied by pores represents 3.6 % for green mold castings. The porosity values for castings from thermally treated binder jetting molds were lower; the lowest porosity value was obtained for samples manufactured from the T2 thermally treated mold. As seen in Section 2.2.4, when the binder jetting molds are thermally treated, the porosity increases, obtaining higher values for higher temperatures. Molds with porosity facilitate the evacuation of gases and prevent defects due to gas porosity. In addition, green molds contain more water and impurities, which generates much more gas during casting compared to thermally treated molds. Therefore, it can be corroborated that the thermal treatment of binder jetting molds positively influences the porosity of castings.

Table 5. Surface porosity of casting specimens.

Thermal-treatment BJ molds	Porosity of castings
Green	3,6%
T1	2,3%
T2	1,3%

4. Conclusions

This research shows that the binder jetting process is useful for manufacturing molds for aluminum alloy castings in industrial applications. The calcium sulfate molds printed by binder jetting process must be thermally treated with a heat cycle to obtain castings with enough quality. The molds should be free of humidity and volatile substances to minimize the generation of gases. In addition, the mold porosity should be enough to facilitate the evacuation of air and gases, minimizing casting defects. These properties are achieved with thermal treatments applied to the binder jetting molds. When the molds are heated, volatile substances are eliminated, and permeability is increased. However, excessive temperature or a too-long heating cycle induces chemical reactions that degrade the material and modify the bonding among particles, reducing the

strength of the mold material. The experiments carried out helped to find the optimum conditions of temperature and time for simultaneously achieving these three objectives (free of water and volatile substances, high porosity and enough mechanical strength to resist the metallostatic pressure exerted by molten metal). A good surface condition and dimensional accuracy are also important in the performance of casting molds. The best mold properties were obtained at 250°C for 1.5 hours (T2 thermal treatment). For this treatment, the binder jetting mold presents the best values for surface roughness, porosity, and compression strength.

In addition, the quality of castings manufactured with different thermally treated molds was studied. For this purpose, aluminum alloy castings were analyzed in terms of dimensional accuracy, surface roughness, mechanical strength, and porosity. On one hand, the results indicate that thermal treatments only very slightly affect dimensional accuracy and roughness. All values are consistent with the traditional sand-casting process. On the other hand, the porosity of castings is affected to a greater extent by thermal treatments of the binder jetting mold. The optimum casting porosity was obtained for the T2 thermal-treatment mold because the gas pores are associated with mold permeability.

Using new methods, based on additive manufacturing, for producing molds opens a promising field of work, characterized by a higher flexibility and savings in time and operating cost.

Acknowledgments.

References

[1] B.P. Conner, G.P. Manogharan, A.N. Martof, L.M. Rodomsky, C.M. Rodomsky, D.C. Jordan, J.W. Limperos, Making sense of 3-D printing: Creating a map of additive manufacturing products and services, Addit. Manuf. 1 (2014) 64–76. https://doi.org/10.1016/j.addma.2014.08.005.

[2] S. Pattnaik, D.B. Karunakar, P.K. Jha, Developments in investment casting process - A review, J. Mater. Process. Technol. 212 (2012) 2332–2348. https://doi.org/10.1016/j.jmatprotec.2012.06.003.

[3] T.A. Le Néel, P. Mognol, J.Y. Hascoët, A review on additive manufacturing of sand molds by binder jetting and selective laser sintering, Rapid Prototyp. J. 24 (2018) 1325–1336. https://doi.org/10.1108/RPJ-10-2016-0161.

[4] R. Singh, R. Singh, Effect of workpiece volume on shell wall thickness reduction in rapid casting of aluminum using three-dimensional printing, Int. J. Automot. Mech. Eng. 6 (2012) 680–691. https://doi.org/10.15282/ijame.6.2012.1.0055.

[5] S.C. Sun, B. Yuan, M.P. Liu, Effects of moulding sands and wall thickness on microstructure and mechanical properties of Sr-modified A356 aluminum casting alloy, Trans. Nonferrous Met. Soc. China (English Ed.) 22 (2012) 1884–1890. https://doi.org/10.1016/S1003-6326(11)61402-7.

[6] H. Shangguan, J. Kang, C. Deng, Y. Hu, T. Huang, 3D-printed shell-truss sand mold for aluminum castings, J. Mater. Process. Technol. 250 (2017) 247–253. https://doi.org/10.1016/j.jmatprotec.2017.05.010.

[7] S.R. Sama, T. Badamo, P. Lynch, G. Manogharan, Novel sprue designs in metal casting via 3D sand-printing, Addit. Manuf. 25 (2019) 563–578. https://doi.org/10.1016/j.addma.2018.12.009.

[8] J. Kang, H. Shangguan, C. Deng, Y. Hu, J. Yi, X. Wang, X. Zhang, T. Huang, Additive manufacturing-driven mold design for castings, Addit. Manuf. 22 (2018) 472–478. https://doi.org/10.1016/j.addma.2018.04.037.

[9] M. Upadhyay, T. Sivarupan, M. El Mansori, 3D printing for rapid sand casting—A review, J. Manuf. Process. 29 (2017) 211–220. https://doi.org/10.1016/j.jmapro.2017.07.017.

[10] D.A. Snelling, C.B. Williams, A.P. Druschitz, Mechanical and material properties of castings produced via 3D printed molds, Addit. Manuf. 27 (2019) 199–207. https://doi.org/10.1016/j.addma.2019.03.004.

[11] M. A. Castro-Sastre, A. I. Fernández-Abia, P. Rodríguez-González, S. Martínez-Pellitero, J. Barreiro, Characterization of materials used in 3d-printing technology with different analysis techniques, Annals of DAAAM Int. 29 (2018) 267-272. https://doi.org/10.2507/29th.daaam.proceedings.136

[12] A. Farzadi, V. Waran, M. Solati-Hashjin, Z.A.A. Rahman, M. Asadi, N.A.A. Osman, Effect of layer printing delay on mechanical properties and dimensional accuracy of 3D printed porous prototypes in bone tissue engineering, Ceram. Int. 41 (2015) 8320–8330. https://doi.org/10.1016/j.ceramint.2015.03.004.

[13] M. Asadi-Eydivand, M. Solati-Hashjin, A. Farzad, N.A. Abu Osman, Effect of technical parameters on porous structure and strength of 3D printed calcium sulfate prototypes, Robot. Comput. Integr. Manuf. 37 (2016) 57–67. https://doi.org/10.1016/j.rcim.2015.06.005.

[14] M. Vaezi, C.K. Chua, Effects of layer thickness and binder saturation level parameters on 3D printing process, Int. J. Adv. Manuf. Technol. 53 (2011) 275–284. https://doi.org/10.1007/s00170-010-2821-1.

[15] N. Coniglio, T. Sivarupan, M. El Mansori, Investigation of process parameter effect on anisotropic properties of 3D printed sand molds, Int. J. Adv. Manuf. Technol. 94 (2018) 2175–2185. https://doi.org/10.1007/s00170-017-0861-5.

[16] P. Patirupanusara, W. Suwanpreuk, T. Rubkumintara, J. Suwanprateeb, Effect of binder content on the material properties of polymethyl methacrylate fabricated by three dimensional printing technique, J. Mater. Process. Technol. 207 (2008) 40–45. https://doi.org/10.1016/j.jmatprotec.2007.12.058.

[17] A. Butscher, M. Bohner, C. Roth, A. Ernstberger, R. Heuberger, N. Doebelin, P. Rudolf Von Rohr, R. Müller, Printability of calcium phosphate powders for three-dimensional printing of tissue engineering scaffolds, Acta Biomater. 8 (2012) 373–385. https://doi.org/10.1016/j.actbio.2011.08.027.

[18] A.W. Fonseca Coelho, R.M. da Silva Moreira Thiré, A.C. Araujo, Manufacturing of gypsum–sisal fiber composites using binder jetting, Addit. Manuf. 29 (2019) 100789. https://doi.org/10.1016/j.addma.2019.100789.

[19] S. Mitra, A. Rodríguez de Castro, M. El Mansori, The effect of ageing process on three-point bending strength and permeability of 3D printed sand molds, Int. J. Adv. Manuf. Technol. 97 (2018) 1241–1251. https://doi.org/10.1007/s00170-018-2024-8.

[20] E. Bassoli, E. Atzeni, Direct metal rapid casting: Mechanical optimization and tolerance calculation, Rapid Prototyp. J. 15 (2009) 238–243. https://doi.org/10.1108/13552540910979758.

[21] ISO 4288:1996 standard, Geometrical Product Specifications (GPS) — Surface texture: Profile method — Rules and procedures for the assessment of surface texture, (1996).

[22] ASTM C373-88, Standard Test Method for Water Absorption, Bulk Density, Apparent Porosity, and Apparent Specific Gravity of Fired Whiteware Products, (2006).

[23] ISO 679:2009 standard, Cement - Test methods - Determination of strength, (2009).

[24] V.S. Ramachandran, R. M.Paroli, J.J. Beandoin, and A.H. Delgado. Handbook of Thermal Analysis of Construction Materials, William Andrew, 2002.

[25] A. Sanitas, N. Coniglio, M. Bedel, M. El Mansori, Investigating surface roughness of ZE41 magnesium alloy cast by low-pressure sand casting process, Int. J. Adv. Manuf. Technol. 92 (2017) 1883–1891. https://doi.org/10.1007/s00170-017-0283-4.

[26] K. Nyembwe, D.J. de Beer, J.G. van der Walt, S. Bhero, Assessment of surface finish and dimensional accuracy of tools manufactured by metal casting in rapid prototyping sand moulds, South African J. Ind. Eng. 23 (2012) 130–143. https://doi.org/10.7166/23-3-516.

[27] M. Asadi-Eydivand, M. Solati-Hashjin, A. Fathi, M. Padashi, N.A. Abu Osman, Optimal design of a 3D-printed scaffold using intelligent evolutionary algorithms, Appl. Soft Comput. J. 39 (2016) 36–47. https://doi.org/10.1016/j.asoc.2015.11.011.

[28] R. Singh, M. Verma, Investigations for deducing wall thickness of aluminium shell casting using three dimensional printing, J. of Achievements in materials and manufacturing eng.32 (2008) 565-569. http://jamme.acmsse.h2.pl/papers_vol31_2/31259.pdf

[29] ISO 6892-1:2016 - Metallic materials — Tensile testing — Part 1: Method of test at room temperature, (2016).

[30] S. Kalpakjian, S. Schmid, Manufacturing Engineering & Technology, 7th ed., Pearson, 2014.

[31] UNE-EN 1706:2011, Aluminium and aluminium alloys - Castings - Chemical composition and mechanical properties, (2011)

[32] C. Tekmen, I. Ozdemir, U. Cocen, K. Onel, The mechanical response of Al-Si-Mg/SiCp composite: Influence of porosity, Mater. Sci. Eng. A. 360 (2003) 365–371. https://doi.org/10.1016/S0921-5093(03)00461-1.

[33] H. Cao, M. Hao, C. Shen, P. Liang, The influence of different vacuum degree on the porosity and mechanical properties of aluminum die casting, Vacuum. 146 (2017) 278–281. https://doi.org/10.1016/j.vacuum.2017.09.048.